

Investigation of the Preparation and Characterization of Fe-doped TiO₂ Nanoparticles

Sagadevan S*

Department of Physics, Sree Sastha Institute of Engineering and Technology, Chennai-600 123, India

Abstract

Fe-doped TiO₂ nanoparticles were synthesized by sol-gel method. The synthesized nanopowders were characterized by powder X-ray diffraction (XRD), Scanning Electron Microscope (SEM), Transmission Electron Microscopy (TEM), Ultraviolet Visible (UV-Vis) and Dielectric studies. The crystallite size and phase were determined by X-ray diffraction (XRD) analysis. The morphology and particle size were studied using the scanning electron microscope (SEM) and transmission electron microscopy (TEM). There is a slight variation in numerical value of crystallite size measured by the two techniques: TEM and XRD peak broadening. The optical properties were obtained from UV-Vis absorption spectrum. The UV-Vis absorption spectrum demonstrated an absorption shift in Fe-doped TiO₂ nanoparticles to longer wavelengths, thus showing an enhancement of the absorption in the visible spectrum. The dielectric studies were carried out at different frequencies and at different temperatures for the prepared Fe-doped TiO₂ nanoparticles. The frequency dependence of the dielectric constant and dielectric loss is found to decrease with an increase in the frequency at different temperatures.

Keywords: Fe-doped TiO₂ Nanoparticles; XRD; SEM; TEM; Dielectric studies

Introduction

In recent years, intense effect was focused on preparation of metal oxide nano crystals due to their noticeably different physical and chemical properties with respect to the bulk materials. Titanium dioxide (TiO₂) is of enormous attention in technological applications due to its morphology and crystalline phase. TiO₂ has been broadly considered regarding various applications, utilizing the photo catalytic and transparent conductivity, which strongly depend on the crystalline structure, morphology and crystallite size [1-3]. Sol-gel is one of the most exploited techniques; it is used mostly to produce thin film and powder catalysts. Many studies revealed that different variants and modifications of the process were used to create pure thin films or powders in large homogeneous concentration and under stoichiometry-control [4]. Sol-gel technology finds applications in the development of new materials for catalysis [5-7], chemical sensors [8], membranes [9], fibers [10], optical gain media [11], photochromic applications [12] and solid state electrochemical devices [13], and in a diverse range of scientific and engineering fields, such as ceramic industry, nuclear industry [14], and electronic industry [15]. In the present investigation, we report the synthesis and characterization of Fe-doped TiO₂ nanoparticles by the sol-gel method. The prepared Fe-doped TiO₂ nanoparticles are characterized by X-ray diffraction, scanning electron microscopy (SEM), transmission electron microscopy (TEM) and UV analysis. The dielectric properties for Fe-doped TiO₂ nanoparticles such as dielectric constant and dielectric loss have been studied as a function of frequency and different temperatures.

Experimental Procedure

Titanium (IV) isopropoxide, ferric chloride has been used as starting materials and ethanol was used as solvent. Initially, titanium (IV) isopropoxide was dissolved in ethanol, mixed with ferric chloride by stirring for 30 min at room temperature and followed by adding droplets of ammonia into the solution. Finally, distilled water was slowly added to the solution by stirring for 30 min. The solution was dried at 120°C for 24 h and calcined at the temperature 500°C for 3 h to obtain Fe-doped TiO₂ nanopowder.

Material Characterization

The XRD pattern of the Fe-doped TiO₂ nanoparticles was recorded by using a powder X-ray diffractometer (Schimadzu model: XRD 6000 using CuKα (λ=0.154 nm) radiation, with a diffraction angle between 10° to 80°. The crystallite size was determined from the broadenings of corresponding X-ray spectral peaks by using Debye Scherrer's formula. Scanning Electron Microscopy (SEM) studies were carried out on JEOL, JSM-67001. The optical absorption spectrum of the Fe-doped TiO₂ nanoparticles has been taken by using the VARIAN CARY MODEL 5000 spectrophotometer in the wavelength range of 200–800 nm. The dielectric properties of the Fe-doped TiO₂ nanoparticles were analyzed using a HIOKI 3532-50 LCR HITESTER over the frequency range 50 Hz-5 MHz.

Results and Discussion

Structural analysis

X-ray diffraction is a most common technique for the study of crystal structures and atomic spacing. The material has been identified, X-ray crystallography may be used to determine its structure, average particle size, unit cell dimensions and sample purity. The X-ray diffraction patterns of Fe-doped TiO₂ nanoparticles are shown in Figure 1. All the observed peaks could be indexed according to the tetragonal structure of TiO₂. The broad peaks indicate either particles of very small crystalline size, or particles are semi crystalline in nature [16]. The average nano-crystalline size (D) was calculated using the Debye-Scherrer formula,

*Corresponding author: Sagadevan S, Department of Physics, Sree Sastha Institute of Engineering and Technology, Chennai-600 123, India, Tel: 044 2681 0114; E-mail: sureshsagadevan@gmail.com

Received March 19, 2015; Accepted April 08, 2015; Published April 16, 2015

Citation: Sagadevan S (2015) Investigation of the Preparation and Characterization of Fe-doped TiO₂ Nanoparticles. J Material Sci Eng 4: 164. doi:10.4172/2169-0022.1000164

Copyright: © 2015 Sagadevan S. This is an open-access article distributed under the terms of the Creative Commons Attribution License, which permits unrestricted use, distribution, and reproduction in any medium, provided the original author and source are credited.

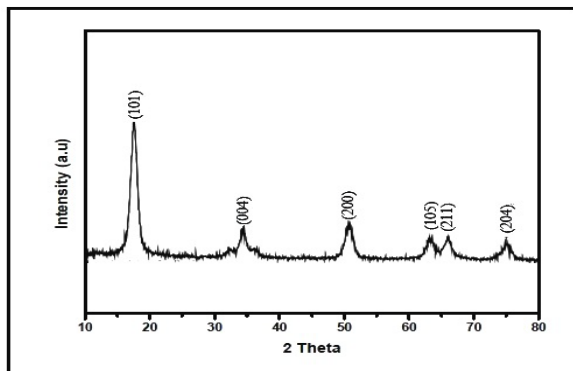


Figure 1: XRD spectrum of Fe-doped TiO₂ nanoparticles.

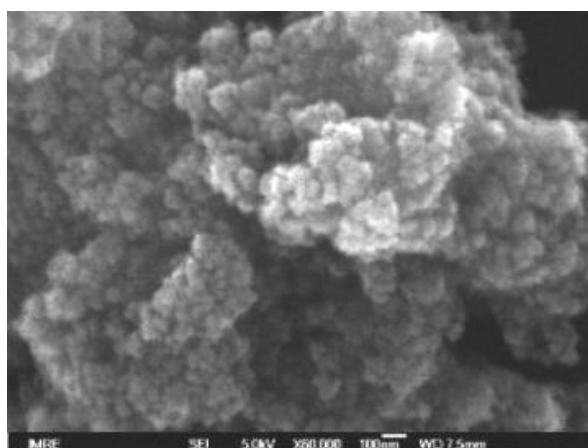


Figure 2: SEM Image of the Fe-doped TiO₂ nanoparticles.

$$D = \frac{0.9\lambda}{\beta \cos \theta} \quad (1)$$

where λ is the X-ray wavelength (CuK α radiation and equals to 0.154 nm), θ is the Bragg diffraction angle, and β is the FWHM of the XRD peak appearing at the diffraction angle θ . The average crystalline size is calculated from X-ray line broadening using Debye-Scherrer equation to be about 15.2 nm which agrees well with the reported value of 15 nm [17].

Scanning Electron Microscopy (SEM) analysis

External morphology, chemical composition, crystalline structure and orientation of materials making up the sample are revealed by SEM. The morphology of the Fe-doped TiO₂ nanoparticles is shown in Figure 2. It presents the clear evidence that of the particles, uniform sized particles are spherical in shape. The image reveals that the average size of the particles is 14.3 nm which is good agreement with reported values of the average size was about 10-15 nm [18].

Transmission Electron Microscopy (TEM)

TEM is commonly used for imaging and analytical characterization of the nanoparticles to assess the shape, size, and morphology. The transmission electron microscopic analysis was carried out to confirm the actual size of the particles, their growth pattern and the distribution

of the crystallites. Figure 3 depicts TEM photograph for the synthesized Fe-doped TiO₂ nanoparticles that proves formation of nanoparticles. Shape of crystallites is spherical in Fe-doped TiO₂ nanoparticles. It is evident from the micrographs that the average size of the particles as directly measured from the image is ~14 nm. The different numerical value of particle size is obtained for the Fe-doped TiO₂ nanoparticles from XRD and TEM technique.

UV-Visible absorption spectrum

Optical absorption measurement was carried out on Fe-doped TiO₂ nanoparticles. Figure 4 shows the variation of the optical absorbance with the wavelength of the as prepared Fe-doped TiO₂ nanoparticles. The optical absorption coefficient has been calculated in the wavelength range of 200 - 800 nm. The absorption edge has been obtained at a shorter wavelength. The broadening of the absorption spectrum could be due to the quantum confinement of the nanoparticles. The UV-Vis spectrum of the Fe doped-TiO₂ nanoparticles show the shift of the wavelength maximum towards the red light zone and this shift depends on the iron content in the lattice [19].

Dielectric studies

The dielectric constant and the dielectric loss of the Fe-doped TiO₂ nanoparticles were studied at different temperatures using the HIOKI 3532 LCR HITESTER in the frequency region 50 Hz-5 MHz. The dielectric constant was measured as a function of the frequency at

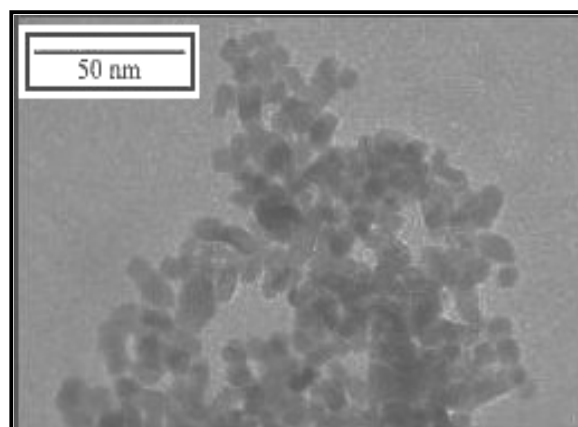


Figure 3: TEM image of Fe-doped TiO₂ nanoparticles.

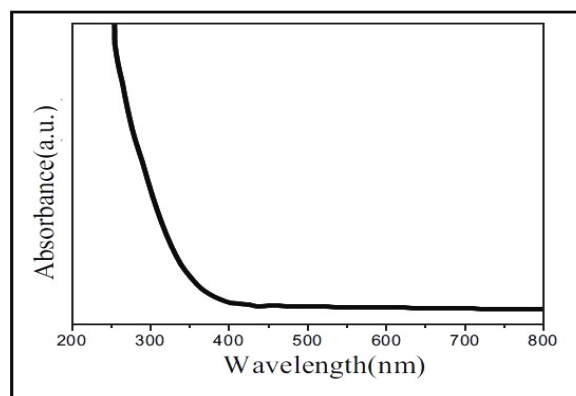


Figure 4: Optical absorbance spectrum of Fe-doped TiO₂ nanoparticles.

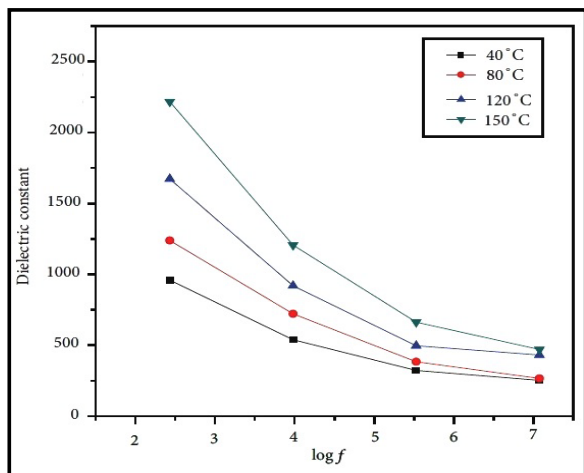


Figure 5: Variation of the dielectric constant against log f.

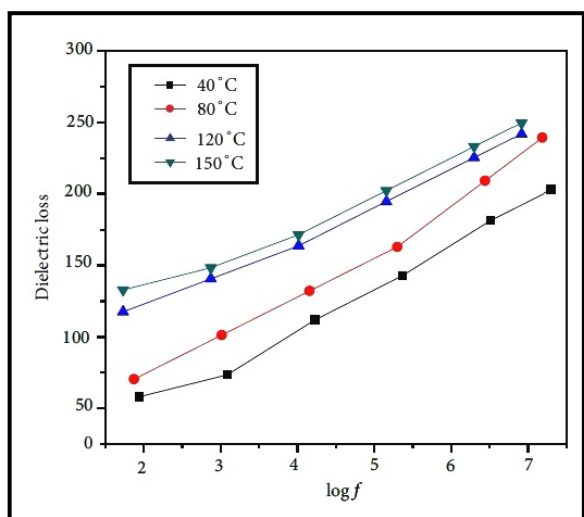


Figure 6: Variation of the dielectric loss with log f.

different temperatures as shown in Figure 5, while the corresponding dielectric losses are depicted in Figure 6. Figure 5 shows the plot of the dielectric constant (ϵ_r) versus applied frequency. It is observed Figure 5 that the dielectric constant decreases exponentially with increasing frequency and then attains almost a constant value in the high frequency region. Fe content TiO₂ nanoparticles show exceptionally high values of dielectric constant at very low frequencies. This value decreases continuously as the frequency is increased. The value of dielectric constant for Fe doped TiO₂ nanoparticles at low frequency [20]. This also shows that the value of the dielectric constant increases with an increase in the temperatures. The involvement of the decrease in the dielectric constant due to electronic polarization is quite less. Dipolar polarization is also predictable to decrease with temperature as it is inversely proportional to temperature. The contribution to polarizability of the space charge depends on the purity of the nanoparticles. At low temperature and high frequency, we may take it as small. However, it is significant in the low frequency region. As the temperature increases, the contribution of the space charge effect towards polarization may have a tendency to increase [21]. The dielectric loss considered as a

function of frequency at different temperatures is shown in Figure 6. These curves suggest that the dielectric loss is strongly dependent on the frequency of the applied field, similar to that of the dielectric constant. Dielectric loss is observed at very low frequencies which gradually decrease towards stable value with the increase in frequency in Fe doped TiO₂ nanoparticles [20]. The dielectric loss decreases with an increase in the frequency at almost all temperatures, but appears to achieve saturation in the higher frequency range of 1 MHz and above, at all the temperatures. In the low frequency region, high energy loss is observed, which may be due to the dielectric polarization, space charge and rotation direction polarization occurring in the low frequency range [22].

Conclusion

Fe-doped TiO₂ nanoparticles have been synthesized using the sol-gel method. The formation of Fe-doped TiO₂ nanoparticles was confirmed by X-ray diffraction (XRD). The size and morphology of the samples were characterized using scanning and transmission electron microscopy (SEM and TEM). The SEM analysis reveals that the morphology of Fe doped TiO₂ was smooth and well defined spherical shape with grain size 14.3 nm. The size of the Fe-doped TiO₂ nanoparticles was characterized using transmission electron microscopy (TEM). The transmission electron microscopic analysis confirms the prepared Fe-doped TiO₂ nanoparticles with the particle size of around 14 nm. The optical properties were studied by the UV-Vis absorption spectrum. The UV-Visible shows Fe doped titanium nanoparticles extend the absorption edge to the visible light range and make the red shift more distinct. The variation of dielectric constant and dielectric loss with frequency and temperature for Fe-doped TiO₂ nanoparticles were analyzed. Initially, the dielectric constant decreases with the increase in frequency and stabilises to a constant value at higher frequencies.

References

- Joseph Antony Raj K, Vishwanathan B (2009) Effect of surface area, pore volume and particle size of P25 titania on the phase transformation of anatase to rutile. *Indian J Chem* 48: 1378-1382.
- Gang L, Xuewen W, Zhigang C, Hui-Ming C, Gao Qing L (2009) The role of crystal phase in determining photocatalytic activity of nitrogen doped TiO₂. *Colloid Interface Sci* 329: 331-338.
- Nakano H, Hasuike H, Kisoda K, Nishio K, Isshiki T, et al. (2009) Synthesis of TiO₂ nanocrystals controlled by means of the size of magnetic elements and the level of doping with them. *J Phys Condens Matter* 21: 064214.
- Bu S, Jin Z, Liu X, Yin T, Cheng Z (2006) Preparation of nanocrystalline TiO₂ porous films from terpeneol-ethanol-PEG system. *J Mater Sci* 41: 2067-2073.
- Oye G, Glomm WR, Vralstad T, Volden S, Magnusson H, et al. (2006) Synthesis, functionalisation and characterisation of mesoporous materials and sol-gel glasses for applications in catalysis, adsorption and photonics. *Adv Colloid Interface Sci* 123-126: 17-32.
- Arnelao L, Barreca D, Moraru B (2003) A molecular approach to RuO₂-based thin films: sol-gel synthesis and characterization. *J Non-Crystal Solids* 316: 364-371.
- Aegerter MA (2001) Sol-gel niobium pentoxide: A promising material for electrochromic coatings, batteries, nanocrystalline solar cells and catalysis. *Sol. Energy Mater. Sol. Cells* 68:401-422.
- Maduraiveeran G, Ramaraj R (2007) A facile electrochemical sensor designed from gold nanoparticles embedded in three-dimensional sol-gel network for concurrent detection of toxic chemicals. *Electrochem Commun* 9: 2051-2055.
- Brinker CJ, Raman NK, Logan MN, Sehgal R, Assink RA, et al. (1995) Structure-property relationships in thin films and membranes. *J Sol-gel Sci Technol* 4: 117-133.
- Zeng ZR, Qiu WL, Huang ZF (2001) Solid-Phase Microextraction Using Fused-

- Silica Fibers Coated with Sol-Gel-Derived Hydroxy-Crown Ether Anal Chem 73: 2429.
11. Jeronimo PCA, Araujo AN, Conceica M, Montenegro BSM (2007) Optical sensors and biosensors based on sol-gel films. *Talanta* 72: 13-27
 12. Volkan M, Stokes DL, Vo-Dinh T (2005) A sol-gel derived AgCl photochromic coating on glass for SERS chemical sensor application. *Sensors Actuators B: Chem* 106: 660-667.
 13. Dunn B, Farrington GC, Katz B (1994) Sol-gel approaches for solid electrolytes and electrode materials. *Solid State Ionics* 70-71: 3-10.
 14. Brinker CJ, Scherer GW (1990) *Sol-gel Science: The Physics and Chemistry of Sol-gel Processing*. Academic Press, Boston, MA.
 15. Phani AR, Passacantando M, Santucci S (2007) Synthesis and characterization of hafnium oxide and hafnium aluminate ultra-thin films by a sol-gel spin coating process for microelectronic applications. *J Non-Crystal Solids* 353: 663-669.
 16. Yeh CL, Yeh SH, Ma HK (2004) Flame synthesis of titania particles from titanium tetraisopropoxide in premixed flames. *Powder Technol* 145: 1-9.
 17. Stoyanova AM, Hitkova HY, Ivanova NK, Bachvarova-Nedelcheva AD, Iordanova RS, et al. (2013) Photocatalytic and antibacterial activity of Fe-doped TiO₂ nanoparticles prepared by nonhydrolytic sol-gel method *Bulgarian Chemical Communications* 45: 497-504.
 18. Kim HJ, Jeong KJ, Bae DS, Kor (2012) *J Mater Res* 22: 5
 19. Luu CL, Nguyen QT, Ho ST (2010) *Adv Nat Sci Nanosci Nanotechnol* 1: 015008.
 20. Singh D, Yadav P, Singh N, Kant C, Kumar M (2013) Dielectric properties of Fe-doped TiO₂ nanoparticles synthesised by sol-gel route. *Journal of Experimental Nanoscience* 8: 171-183.
 21. Suresh S, Aruneshan C (2014) Dielectric Properties of Cadmium Selenide (CdSe) Nanoparticles synthesized by solvothermal method. *Appl Nanosci* 4: 179-184.
 22. Sagadevan S (2014) Studies on the dielectric properties of CdS nanoparticles. *Appl Nanosci* 4: 325-329.